Lead-acid battery modeling over full state of charge and discharge range

A. Azzollini et al.

Lead-Acid Battery Modeling Over Full State of Charge and Discharge Range

In:

IEEE Transactions on Power Systems, vol. 33, no. 6, pp. 6422-6429, Nov. 2018

The final published version is available online at:

https://doi.org/10.1109/TPWRS.2018.2850049

Lead-Acid Battery Modeling over Full State of Charge and Discharge Range

Ilario Antonio Azzollini, Valerio Di Felice, Francesco Fraboni, Lorenzo Cavallucci, Marco Breschi, *Senior Member, IEEE*, Alberto Dalla Rosa, and Gabriele Zini

***Abstract*—The discharge behavior of electrochemical solid state batteries can be conveniently studied by means of electrical analogical models. This paper builds on one of the best known models proposed in literature for lead-acid electrochemistry (the Ceraolo's model) by formulating an alternative third-order model and implementing a methodology to compute all model parameters (using particle swarm and non-linear programming optimization) with increased precision and full usability over the whole range of possible states of charge and discharge currents. The developed methodology is used efficiently to model all commercial lead-acid batteries and enable their integration into simulation software for the optimized design of energy systems using energy storage.**

***Index Terms*—Battery modeling, energy storage, lead-acid battery, non-linear programming, optimization, particle swarm optimization.**

I. Introduction

LEAD-ACID batteries are the most widespread rechargeable electrochemical devices, used in many different applications to guarantee quality of service even in absence of a power source for reasonably long periods of time. To better design and evaluate complex systems resorting to lead-acid energy storage for correct functioning, reliable and precise battery models are needed.

A number of different modeling strategies can be adopted for energy storage characterization [1]. *Natural* models aim at devising an accurate, usable, and reproducible physical-chemical framework that explains the natural phenomena occurring during the functioning of the batteries; such models are translated into sets of equations that are used to evaluate the variation of the battery parameters during functioning. *Empirical* modeling is based on descriptions of the observed data, frequently employing regression analysis or artificial intelligence techniques to model the response of the battery from a set of input variables. *Abstract* models use analogies (normally with electrical circuits or stochastic process models) that simplify the real behavior of the system but improve the capability to interpret and understand the way the battery works. *Mixed* models combine the advantages of the previous strategies to obtain more refined results while retaining a reasonably simplified model.

Natural models are normally developed by experts in electrochemistry [2]–[9]; the complexity that is inherent in this modeling technique is hampering its efficient use for commercial purposes. This gives way to abstract or mixed models [10], [11] which have proved to be more readily usable, although less stringent from a scientific point of view. In particular, mixed models based on electrical circuit parametrization can be more easily implemented in electrical simulation codes that are already designed to deal with the input and output variables typical of battery technology (namely, voltage and current). As a matter of fact, the third-order dynamical model developed in [11] for lead-acid batteries has been implemented in a package of a well-known commercial mathematical software [12]. Electrochemical batteries are indeed conveniently modeled by means of electrical analogy, i.e. using networks of well-known electrical components (resistors, capacitors, electromotive forces, etc.); in literature, two different approaches can be found: modeling every single part of the battery with a corresponding electrical element [13], [14], or modeling the battery behavior by using a black box approach interpreting what is the output at the terminals of the battery [15]–[17].

An example of abstract battery modeling by means of artificial intelligence techniques can be found in [18], where fuzzy logic is employed to characterize the discharge of lead-acid batteries by modeling the relationship between the battery open-circuit voltage, the state of charge, and the discharge currents.

A general model structure for lead-acid batteries was defined by Ceraolo in [11], from which specific models can be inferred, and in particular, the implementation of the third-order model was developed in detail. In the context of the general framework proposed by Ceraolo, an alternative third-order model formulation is presented in this paper, showing an extended validity and usability over all the State Of Charge (SOC) and discharge current ranges. Compared to Ceraolo's third-order model formulation, a resistance is added to the main branch, whose characteristic equation is designed for fitting as close as possible the lead-acid battery behavior at the beginning of the discharge process. Then, as the model is characterized by a significant number of parameters to be identified, an optimization methodology is proposed and tested on a battery commercial data-sheet. The overall result is a complete, fully functional, and easily usable methodology that can be implemented as a library for further integration into other advanced energy systems' simulation software.

The paper is organized as follows. Section II describes the model modification and the parameter evaluation for the correct characterization of the battery at all current rate discharging over the full SOC range with comparison between modeled and real curves. Section III discusses the main results and draws the main conclusions. The Appendix describes the original third-order model adopted for this study.

II. Model modification and methodology for parameter estimation

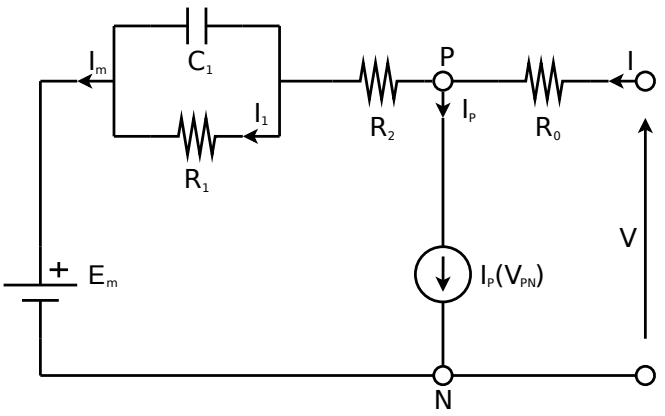

Fig. 1: Lead-acid battery third-order model equivalent circuit from [11].

The starting point of this work is the lead-acid battery third-order dynamical model developed in [11], which is an abstract model for the characterization of the battery operation. The equivalent electric network representing this model is shown in Fig. 1, where:

- E_m is the open-circuit voltage of the battery;
- R_0 accounts for the internal resistance of the battery;
- the R_1-C_1 parallel network models the transient behavior of the battery;
- I is the discharge current of the battery (in Fig. 1 the charge current directions are indicated by the arrows);
- V is the output voltage of the battery;
- the parasitic reaction branch models non-reversible reactions occurring from water electrolysis at end of charge.

The behavior of the parasitic branch is highly non-linear and is modeled as a voltage controlled current source. The parasitic branch is introduced together with R_2 only to model the charging process [1]. The network in Fig. 1 is included in the general model structure for lead-acid batteries presented in [11], in which, any number of R-C blocks can be included in the main branch to achieve the desired accuracy. In the third-order formulation from [11], two R-C blocks are used (with $C_2 = 0$).

The equations governing the circuit model shown in Fig. 1 are described in Appendix A. Apart from the many merits of this model, the main drawback is the fact that it does not allow a precise reproduction of the initial voltage evolution at discharge, showing a rather large difference with respect to the measured discharge curves, as shown in Fig. 2 (for a 0.1 C discharge rate[2]). To solve this discrepancy, a resistance can be added in series with the main branch. The value of this new resistance must depend on SOC, as it needs to grow

[1]For the sake of simplicity, the work outlined in this paper focuses only on the characterization of battery discharge, where the parasitic branch and the resistance R_2, used in [11] for charging modeling, are not discussed although are maintained in our modified model.

[2]It is common norm to express the discharge current as a function of the nominal battery capacity C, expressed in Ah. As an example, the discharge current 1C is the current (in Amps) for which the battery is completely discharged in one hour.

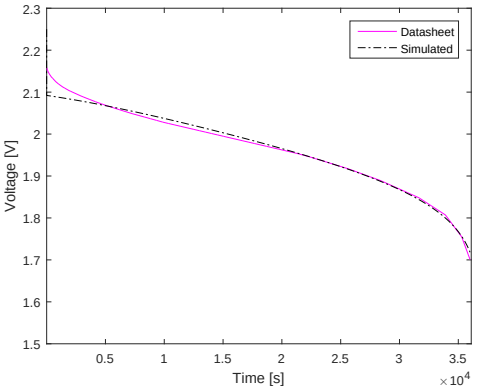

(a)

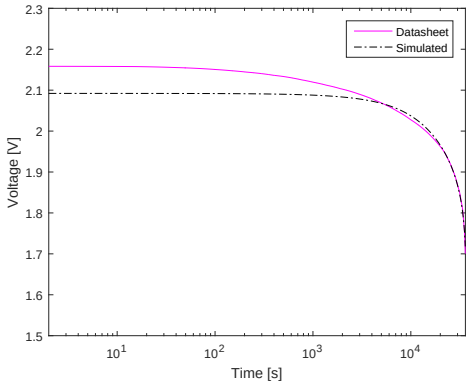

(b)

Fig. 2: 0.1C curve using the model from [11]: (a) linear scale and (b) log scale.

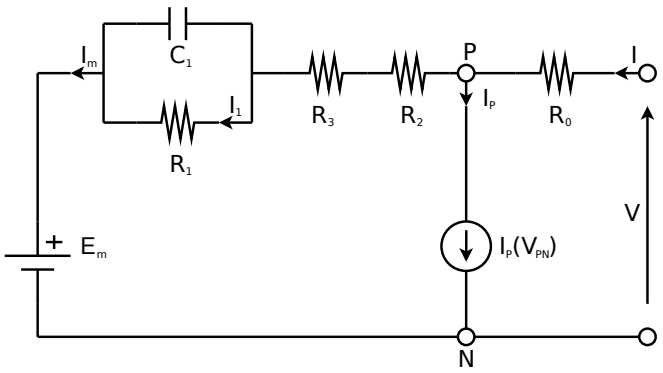

Fig. 3: Modified lead-acid battery equivalent network.

exponentially only at the beginning of the discharge process and then settle to a constant value. The formulation of this additional network component was designed to be as follows

$$R_3 = R_{30}\left\{1 - \exp\left[A_{31}\left(1 - SOC\right)\right]\right\} \tag{1}$$

where R_{30} and A_{31} are constants that depend on the battery technology and therefore must be evaluated from the datasheet of the specific battery to be modeled. The modified third-order model lead-acid battery equivalent network, able to precisely follow the profile of the initial voltage, is shown in Fig. 3. The proposed network is still included in the general model structure presented in [11], as the addition of R_3 in the

main branch can be seen as the addition of an R-C block with $C_3 = 0$. It should be also noted that the resulting model is still a third-order one, as no dynamic circuit elements are added to the original third-order model formulation.

All model parameters need to be estimated to correctly simulate the behavior of the battery over the full range of different discharge current rates. This is achieved by employing fitting algorithms that find the best parameter values to minimize the difference between the modeled and the real discharge curves.

Since the model is characterized by a large number of parameters that have to be evaluated during the modeling process, a sensitivity analysis was performed in order to single out which parameters have the largest effect on the model output. Some parameters hence can be considered as constants, either because they have a definite electrochemical meaning, or because their influence on the output voltage is negligible with respect to other parameters. Therefore, the identification of the parameters with the largest effect on the output is intended as a strategy to reduce the total number of parameters to be fed into the fitting algorithm.

First of all, as the aforementioned resistance R_3 (in (1)) is the only component able to properly model the beginning of the discharge, no sensitivity analysis will be performed on the parameters R_{30} and A_{31}. Then, referring to the model equations presented in Appendix A, the parameters that can be approximated with constant values are the following:

- the reference current I^* and the nominal capacity C_0^* that can be fixed to the values found in the data-sheet;
- the ambient temperature θ_a, that can be fixed to the corresponding real value;
- the freezing electrolyte temperature θ_f, that can be fixed to $-40°$C for lead-acid battery type;
- the battery open-circuit voltage at full charge E_{m0}, that can be fixed to the corresponding real value;
- the battery internal resistance at full charge R_{00} was found to be dependent on the discharge current but it can be easily calculated using the following:

$$R_{00} = \frac{(E_{m0} - V)}{I} \tag{2}$$

where I is the discharge current and V is the battery voltage at the beginning of the discharge process when the battery is fully charged. As soon as the discharge current starts flowing, the battery voltage drops from E_{m0} to V almost instantaneously. This means that V can be chosen as the first voltage measurement available on the data-sheet. In the data-sheet used in this work, the first voltage measurement was taken after 1 second from the beginning of the discharge.

The sensitivity analysis was performed on the remaining parameters using the output voltage profile from [11] as a reference; when one parameter is changed, the difference between the new output voltage values and the reference is computed, as per:

$$\Delta = \sqrt{\frac{\sum_{i=0}^{N}(V_i^{ref} - V_i^{new})^2}{N}} \tag{3}$$

This Δ is nothing but a Root Mean Square Error (RMSE), where:

- V_i^{ref} is the reference voltage value at the point i;
- V_i^{new} is the new output voltage value at the point i;
- N is the total number of points considered, equal to the discharge time in seconds.

For the sake of example, the sensitivity analysis for R_{10} is shown in Fig. 4, where R_{10} varies in the range from -90% to $+90\%$ of its reference value, with a resulting error map shown in Table I. The results of the sensitivity analysis show that:

- the battery thermal capacitance C_θ and thermal resistance R_θ can be excluded from the fitting process because they have a small impact on voltage;
- ϵ and K_E can be fixed since they have only an impact on the temperature-based behavior that is not significant in the data-sheet curves;
- the time constant τ_1 can be fixed since it is a key factor in the charging curve which is not the objective of the optimization;
- since both δ and K_C have an impact on the available capacity of the battery, it is possible to fix one and fit only the other;
- A_0, R_{10}, K_C have a remarkable impact on the voltage behavior and will be the objective of the fitting process.

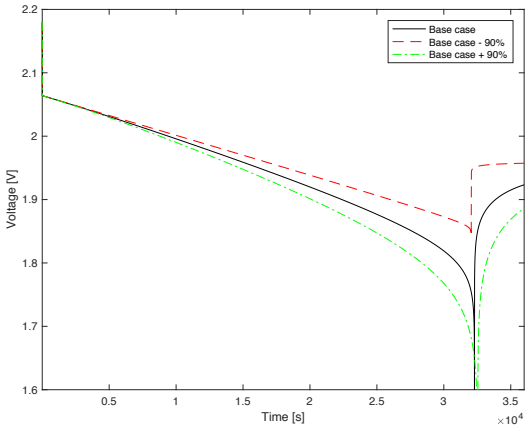

Fig. 4: Study of the influence of the parameter R_{10} on the output voltage, for variations of $\pm 90\%$ of the reference value.

TABLE I: Overview of the error values corresponding to variations from -90% to $+90\%$ of the parameter R_{10}

Variation	Δ[V]	Variation	Δ[V]
-10%	0.0057	+10%	0.0069
-20%	0.0095	+20%	0.0099
-30%	0.0134	+30%	0.0137
-40%	0.0175	+40%	0.0182
-50%	0.0214	+50%	0.0222
-60%	0.0253	+60%	0.0265
-70%	0.0292	+70%	0.0305
-80%	0.0334	+80%	0.0346
-90%	0.0373	+90%	0.0386

In order to find the parameters of the equivalent electrical model described so far, a fitting process that entails a two-step approach was developed and applied to each discharge curve.

The first step focuses on the first half of the discharge curve only, and is devised to obtain an accurate value of R_{30} (introduced, as previously discussed, to better model the initial phase of the discharge curve). The output of this step also gives an initial estimate of the other parameters of the model. The second step uses as starting point the output solution of the previous step (without R_{30}), with the goal of refining the pre-solution output of the first step; this time the evaluation function of this second part is different from the previous one since it considers the whole curve and not only the first half.

For the first step, a *Particle Swarm Optimization* (PSO, see [19]) algorithm is initially applied to the fitting problem; after the PSO has found the initial set of data, a further fine-tuning is performed on such data set by means of a non-linear programming algorithm which works more efficiently over the smaller solution interval range already identified by the PSO. The second step employs a non-linear programming algorithm working over the starting point as output by the first step.

The first action required to start the fitting process is choosing the set of parameters' upper and lower bounds to avoid unfeasible solutions and long computation times:

- A_{31} and R_{30} play a significant role in determining the behavior of the first part of the voltage curve. A_{31} was considered as a negative value, because when the battery is nearly empty (SOC $\simeq$ 0) the resistance (R_3) will tend to R_{30}, which must be positive;
- K_C is strictly related to the capacity and its value needs to be greater than 1, otherwise the capacity might be less than zero for some discharge current which is physically incorrect;
- R_{10} needs to be positive otherwise the resistance R_1 of the equivalent circuit could assume negative values;
- A_0 cannot be less than -1 otherwise the resistance R_0 of the equivalent circuit could assume negative values.

The selected lower and upper bounds are reported in Table II.

TABLE II: Parameter lower and upper bounds used in the fitting algorithms

Parameter	Lower bound	Upper bound
R_{10}	0 Ω	0.06 Ω
K_C	1.001	2
A_0	-1	3
R_{30}	0 Ω	1E-2 Ω
A_{31}	-25	0

III. Results and Conclusions

In this Section, the results of the optimization process applied to determine the best fit value of the parameters described in the Appendix and in (1) are reported. The fitting methodology was applied on each of the discharge curves made available by the data-sheets. Within the parameter set, R_{10} and A_{31} have shown such narrow variation ranges that they have been set to constant values to reduce the computation time without loss of accuracy. R_{10} and A_{31} values have been chosen from the fitting of the 0.1 C discharge curve and then passed on to the following fitting phases as fixed parameters. Moreover, since K_C can be simplified in (A.1), it is not used for 0.1C discharge curve fitting. Therefore the parameters used for the fitting of this first curve are: R_{10}, A_0, R_{30} and A_{31}. After selecting the constant values for R_{10} and A_{31}, the fitting for the other discharge curves was performed over the remaining parameters: K_C, A_0 and R_{30}. The process described above is represented in Fig. 5.

Some of the constant values used for the fitting have been taken from the data-sheet or calculated as an average of the parameters given in [11] and are shown in Table III. The values found by the fitting algorithm are shown in Table IV.

The results can be graphically appreciated in Fig. 6 and Fig. 7. The differences between the data-sheet curves and the optimized ones have been calculated using (3) and are reported in Table V. The results are satisfactory, as the application of the proposed methodology results to be crucial for reaching this degree of precision. Indeed, the direct application of any heuristic algorithm the authors are aware of, did not give results with the same level of accuracy as those shown in this section. A comparison between our proposed methodology and a direct application of heuristic algorithms is not shown for lack of space.

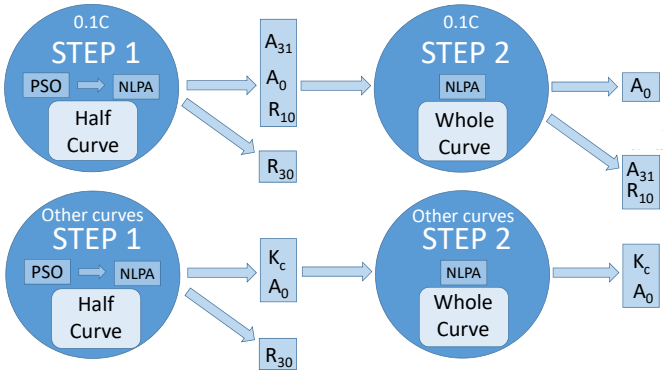

Fig. 5: Schematic of the two fitting steps for the 0.1C (above) and the other discharge curves (below).

TABLE III: Fixed values of the circuit model parameters

Parameter	Value	Parameter	Value
θ_a	20 °C	ϵ	1.24
C_θ	54000 J/°C	K_E	7E-4 V/°C
R_θ	0.2 °C/W	τ_1	6100 s
θ_f	-40 °C	E_{m0}	2.25 V
C_0	540000 As	I^*	15 A
δ	1.575		

TABLE IV: Optimized values of the circuit model parameters

Current	$R_{10}[\Omega]$	K_C	A_0	$R_{30}[\Omega]$	A_{31}	$R_{00}[\Omega]$
0.1C	3.73E-3	-	-0.65	5.04E-3	-18.5	6.11E-3
0.26C	3.73E-3	1.0782	-0.95	1.60E-3	-18.5	2.93E-3
0.68C	3.73E-3	1.0290	-1.00	3.14E-4	-18.5	1.57E-3
1.22C	3.73E-3	1.0831	-0.46	7.6E-5	-18.5	1.24E-3
2C	3.73E-3	1.2401	-0.12	4.6E-5	-18.5	9.17E-4
2.6C	3.73E-3	1.5192	0.44	0	-18.5	8.72E-4

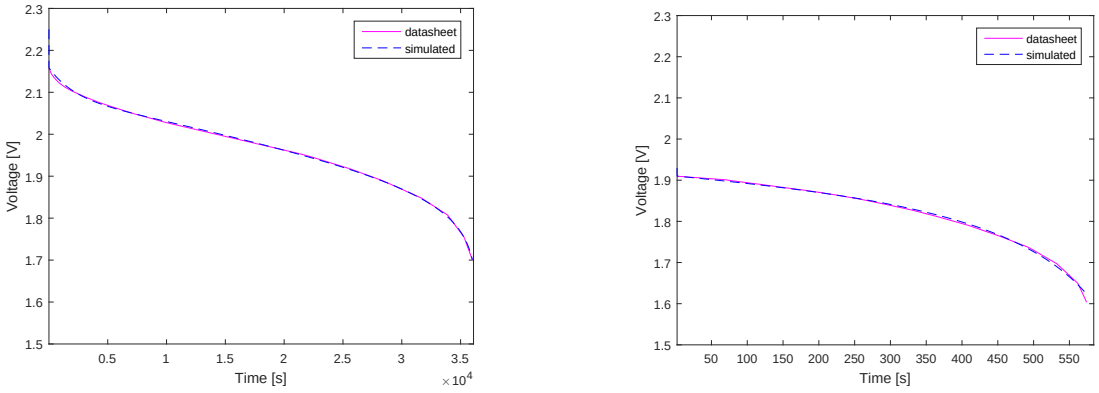

(a) (b)

Fig. 6: Comparison between data-sheet and simulated discharge curves in linear scale: (a) 0.1C curve and (b) 2.6C curve.

TABLE V: Differences between data-sheet curves and optimized curves

Current	Δ[V]
$15A$ (0.1C)	0.0023
$39A$ (0.26C)	0.0077
$102A$ (0.68C)	0.0075
$183A$ (1.22C)	0.0061
$300A$ (2C)	0.0109
$390A$ (2.6C)	0.0145

In Fig. 8 it is highlighted how the proposed model improves on [11] for the 0.1 C discharge curve. Please note that the addition (and optimization) of the network component R_3 is proven to be adequate for the modeling of the initial exponential-like behavior of the voltage curve. This peculiar behavior of the initial voltage is particularly visible for slow discharge current rates.

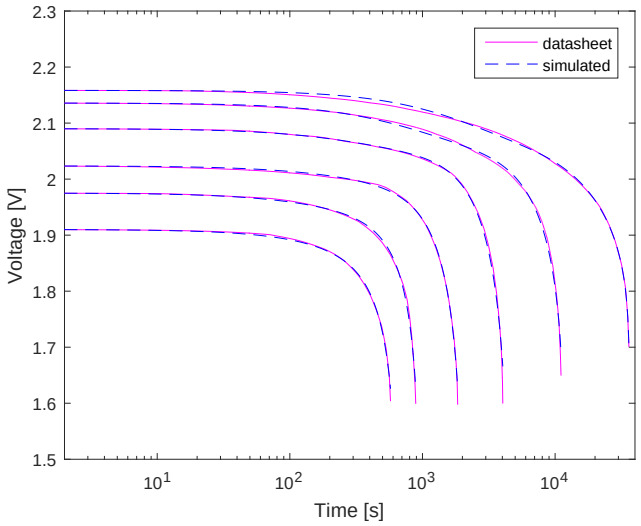

Fig. 7: Comparison between data-sheet and simulated discharge curves in log scale.

At discharge current rates greater than 2.0 C, the initial voltage profile does not exhibit the aforementioned behavior and, in these conditions, Ceraolo's model can reproduce very well the experimental data. This observation is corroborated by the optimized values of the model parameters reported in

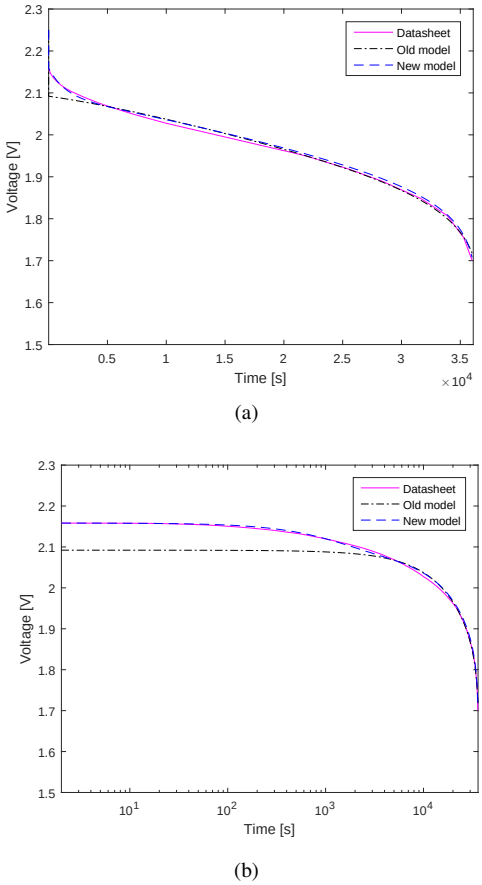

(a)

(b)

Fig. 8: Fitting of the 0.1C curve in (a) linear scale and (b) log scale: comparison between [11] and the new model.

Table IV. As a matter of fact, comparing the values of R_{30} and R_{00}, it can be noticed that the first becomes negligible with respect to the second for the current discharge rate of 2.6 C, but remains significant until the 2.0 C discharge rate. The comparison with [11] is only shown for the 0.1 C discharge current since in this case the difference between the two models can be better appreciated.

The purpose of this work was to accurately model the discharge behavior of lead-acid batteries over the full capacity

range by taking as reference the discharge curves provided by commercially available data-sheets. Starting from the well-known third-order dynamical model in [11], an improvement to the electrical circuit and a fitting algorithm have been proposed to improve the accuracy of the model over the complete set of discharge curves. As a result, it is now possible to use the model with greater accuracy in more comprehensive simulation packages designed for the sizing and analysis of full-fledged energy plants that use batteries as electricity storage devices.

A hybrid optimization methodology was developed, consisting in the combination of particle swarm optimization and non-linear programming minimization algorithm:

- starting from a wide search range, the particle swarm optimization algorithm finds the region in which the minimum is located;
- the non-linear minimization algorithm works in the neighborhood of the minimum and further minimizes the error.

The results are satisfactory as the discharge curves at all current rates are modeled with a negligible error, even when considering the slowest discharge rate that lasts over a period of several hours.

The proposed lead-acid battery model cannot be further tested and improved by using only commercial data-sheets data. Future studies will be performed on the basis of the developments discussed in this paper by taking advantage of more accurate information from direct measurements on batteries subjected to various load profiles taken from real world applications, that will complement the commercial data-sheets discharge curves used so far. The goal is an accurate modeling not only of the discharge process, but also of the battery thermal behavior and charge process. Furthermore, it is also of interest to acquire a better understanding and evaluation of the recovery of capacity phenomena occurring after battery idling or with variable discharge current rates, for lead-acid as well as other battery electrochemical technologies.

APPENDIX A
THIRD-ORDER MODEL DESCRIPTION FROM [11]

The total capacity C is described as follows:

$$C(I,\theta) = \frac{K_C {C_0}^* \left(1 - \frac{\theta}{\theta_f}\right)^{\epsilon}}{1 + (K_C - 1)\left(\frac{I}{I^*}\right)^{\delta}} \tag{A.1}$$

where:

- I is a discharge current (in Amps), in particular:

$$I = I_1 = \frac{I_m}{1 + \tau_1 s} \quad with \quad \tau_1 = R_1 C_1 \tag{A.2}$$

- I^* is a reference current. For instance, the nominal current, defined as the ratio between the nominal capacity and the nominal discharge time;
- θ is the electrolyte temperature (in $^\circ$C);
- θ_f is the electrolyte freezing temperature, usually assumed as equal to $-40\,^\circ$C;
- ${C_0}^* = {C_0}^*(I) = C_0(I^*)$ where $C_0(I)$ is an empirical function of the discharge current and it is equal to the battery capacity at $0\,^\circ$C;
- K_c, ϵ, δ are empirical constant coefficients for a given battery at a given I^*.

The extracted charge Q_e is given by:

$$Q_e(t) = Q_{e\_init} + \int_0^t -I_m(\tau)d\tau \tag{A.3}$$

where the battery is assumed to be completely charged at $t = 0$.

The State Of Charge (SOC) and Depth Of Charge (DOC) are computed using:

$$SOC = 1 - \frac{Q_e}{C(0,\theta)} \tag{A.4}$$

$$DOC = 1 - \frac{Q_e}{C(I_1,\theta)}. \tag{A.5}$$

A uniform value of the electrolyte temperature over its volume θ is used[3] and computed as:

$$C_\theta \frac{d\theta}{dt} = P_s - \frac{(\theta - \theta_a)}{R_\theta} \tag{A.6}$$

where C_θ is the battery overall thermal capacitance, assumed independent from temperature, R_θ is the thermal resistance between the battery and the environment, θ_a is the ambient temperature, and P_s is the internally generated heat of the battery (source thermal power), namely the heating power generated inside the battery by the conversion from chemical to electrical energy and vice-versa.

The electrolyte temperature $\theta(t)$ results in:

$$\theta(t) = \theta_{init} + \int_0^t \frac{P_s - \frac{(\theta - \theta_a)}{R_\theta}}{C_\theta} d\tau \tag{A.7}$$

where θ_{init} is the initial temperature of the battery in $^\circ$C, assumed to be equal to the surrounding ambient temperature.

The main branch voltage E_m comes from:

$$E_m = E_{m0} - K_E(273 + \theta)(1 - SOC) \tag{A.8}$$

where E_{m0} is the open-circuit voltage at full charge, K_E is a constant for the battery under study, and $(273 + \theta)$ is simply the electrolyte temperature in Kelvin.

The terminal resistance R_0 is provided by:

$$R_0 = R_{00}[1 + A_0(1 - SOC)] \tag{A.9}$$

where R_{00} is the value of R_0 at full charge ($SOC = 1$), and A_0 is a constant that depends on the specific battery technology.

The main branch resistance R_1 is computed with:

$$R_1 = -R_{10} \ln(DOC) \tag{A.10}$$

where R_{10} is a constant that depends on the specific battery technology.

[3]The precise characterization of the thermal behavior of the battery entails a-priori knowledge on battery construction, materials, thermal exchanges with the outside environment which is outside the scope of this paper.

The main branch capacitance C_1 is given by:

$$C_1 = \frac{\tau_1}{R_1} \tag{A.11}$$

The dynamic equations of this third-order model are finally the following:

$$\frac{dI_1}{dt} = \frac{1}{\tau_1}(I_m - I_1) \tag{A.12}$$

$$\frac{dQ_e}{dt} = -I_m \tag{A.13}$$

$$\frac{d\theta}{dt} = \frac{1}{C_\theta}\left[P_s - \frac{(\theta - \theta_a)}{R_\theta}\right] \tag{A.14}$$

REFERENCES

[1] D. R. R. Rao, S. Vrudhula, "Battery modeling for energy-aware system design," *Computer*, pp. 77–87, December 2003.

[2] A. B. Ansari, V. Esfahanian, and F. Torabi, "Discharge, rest and charge simulation of lead-acid batteries using an efficient reduced order model based on proper orthogonal decomposition," *Applied Energy*, vol. 173, pp. 152 – 167, 2016.

[3] M. Shepard, "Design of primary and secondary cells, an equation describing battery discharge," *Journal Electrochemical Society*, vol. 112, pp. 657–664, 1965.

[4] K. J. Vetter, *Electrochemical Kinetics*. Elsevier, 1967.

[5] H. Bode, *Lead-Acid Batteries*. J. Wiley & Sons, 1977.

[6] L. Gopikanth and S. Sathyanarana, "Impedance parameters and the state-of-charge," *Journal of Applied Electro-Chemistry*, vol. 9, pp. 369–379, 1979.

[7] G. Smith, *Storage Batteries*. Pitman Advanced Publishing Program, 1980.

[8] J. Gou, A. Lee, and J. Pyko, "Modeling of the cranking and charging processes of conventional valve regulated lead acid (vrla) batteries in micro-hybrid applications," *Journal of Power Sources*, vol. 263, pp. 186 – 194, 2014.

[9] K. Gandhi, "Role of electrical resistance of electrodes in modeling of discharging and charging of flooded lead-acid batteries," *Journal of Power Sources*, vol. 277, pp. 124 – 130, 2015.

[10] K. Sun and Q. Shu, "Overview of the types of battery models," in *Proceedings of the 30th Chinese Control Conference*, July 2011, pp. 3644–3648.

[11] M. Ceraolo, "New dynamical models of lead-acid batteries," *IEEE Transactions on Power Systems*, vol. 15, no. 4, pp. 1184–1190, Nov 2000.

[12] R. A. Jackey, "A simple, effective lead-acid battery modeling process for electrical system component selection," SAE Technical Paper, Tech. Rep., 2007.

[13] S. A. Ilangovan, "Determination of impedance parameters of individual electrodes and internal resistance of batteries by a new non-destructive technique," *Journal of Power Sources*, vol. 50, pp. 33–45, 1994.

[14] H. L. Wiegman and R. Lorenz, "High efficiency battery state control and power capability prediction," in *15th Electric Vehicle Symposium*, vol. 15, 1998.

[15] R. Giglioli, P. Pelacchi, V. Scarioni, A. Buonarota, and P. Menga, "Battery model of charge and discharge processes for optimum design and management of electrical storage systems," in *33rd International Power Source Symposium*, 1988.

[16] R. Giglioli, A. Buonarota, P. Menga, and M. Ceraolo, "Charge and discharge fourth order dynamic model of the lead-acid battery," in *10th International Electric Vehicle Symposium*, 1990.

[17] M. Ceraolo, A. Buonarota, R. Giglioli, P. Menga, and V. Scarioni, "An electric dynamic model of sodium sulfur batteries suitable for power system simulations," in *11th International Electric Vehicle Symposium*, 1992.

[18] C. Burgos, D. Sez, M. E. Orchard, and R. Crdenas, "Fuzzy modelling for the state-of-charge estimation of lead-acid batteries," *Journal of Power Sources*, vol. 274, pp. 355 – 366, 2015.

[19] R. Kennedy, J.; Eberhart, "Particle swarm optimization," in *Proceedings of IEEE International Conference on Neural Networks*, vol. IV, 1995, pp. 1942–1948.

Ilario Antonio Azzollini received the B.S. degree in Automation Engineering from Alma Mater Studiorum University of Bologna, Italy, 2016. He is currently pursuing the M.S. degree in Systems and Control at Delft University of Technology, Delft, Netherlands. His research interest includes nonlinear optimization, nonlinear and adaptive control, and distributed control. During his first bachelor year, Mr. Azzollini was awarded with the Alma-Tong scholarship and therefore he spent the second academic year as an exchange student at Tongji University of Shanghai, China.

Valerio Di Felice was born in Atri, Italy, in 1990. He received B.S. and M.S. in energy and nuclear engineering from University of Bologna in October 2012 and March 2015 respectively. He is currently working as consultant for Amplio Energy and his main research fields are: optimization of photovoltaic plants, electrical storage systems and energy efficiency.

Francesco Fraboni was born in Bentivoglio, Bologna, Italy, in 1995. He received the B.S. degree in Chemical and Biochemical Engineering from Alma Mater Studiorum University of Bologna, in December 2017, where he is also currently pursuing the M.S. degree. His thesis focused on the behavior of lead-acid batteries during charge and discharge processes. Mr. Fraboni was admitted to the Overseas mobility programme by University of Bologna and therefore he is currently spending a semester at Monash University, Melbourne, Australia.

Lorenzo Cavallucci was born in Assisi, Italy, in 1989. He received the B.S and M.S. degree in Energy and Nuclear Engineering from University of Bologna, in October 2011 and March 2014 respectively. He his currently pursuing the Ph.D. degree in Applied Superconductivity at the Department of Electrical, Electronic and Information Engineering Guglielmo Marconi of the University of Bologna. His research interest includes the analysis of quench and the study of electrothermal stability of high temperature and low temperature high field superconductive magnets.

Marco Breschi graduated with honors in electrical engineering from the University of Bologna, Italy, in July 1997. He received his Ph.D. in Electrical Engineering from the University of Bologna in March 2001, with a study on the electrodynamics of superconducting magnets for the Large Hadron Collider of CERN. In 2004 he worked as a visiting scientist at the National High Magnetic Field Laboratory, Florida, USA. Since October 2001 he is Assistant Professor, and since October 2014 he is Associate Professor at the Department of Electrical, Electronic and Information Engineering of the University of Bologna. He is the author or co-author of several multiphysics models for superconducting wires, cables and magnets, based both on FEM and circuit models, developed to investigate the electromagnetic, electrothermal, and electromechanical phenomena of interest for technical applications. His research activity is related to various aspects of magnet technology, applied superconductivity and electrical energy storage. Prof. Breschi is Senior Member of IEEE and served as a Technical Editor for the Special Issues of IEEE Transactions on Applied Superconductivity published after the International Conferences MT22, MT23, MT24, EUCAS 2015, ASC 2016.

Alberto Dalla Rosa spent 11 years in Tokyo, Japan, advising the 16 GW+ utility conglomerate J-Powers in the deregulated electricity generation sectors worldwide, reaching todays equity portfolio of 3,000 MW in the USA and South East Asia. After returning to Europe, he 2 years as VP of International Development in Enelpower (ENEL) and CEO of Archimedes S.r.l. for solar PV investments. Alberto is a mechanical engineer and holds an MBA from the Sloan School of Management at MIT, Boston.

Gabriele Zini has worked for multinational companies (Tetra Pak, Renault-Nissan, Caterpillar, Italcementi Group, Merloni), the Swiss Federal Polytechnic in Zurich (ETH) and the French Nuclear and Renewable Energy Commission (CEA), and is a published author of several peer-reviewed papers and two books: *Solar Hydrogen Energy System - Science and Technology for the Hydrogen Economy*, 2012 by Springer Verlag and *Green Electric Energy Storage Science and Finance for Total Fossil Fuel Substitution*, 2017 by McGraw-Hill. Gabriele holds an Msc in Electronic Engineering, a PhD in Advanced Materials and an MBA from SDA Bocconi, Milan.